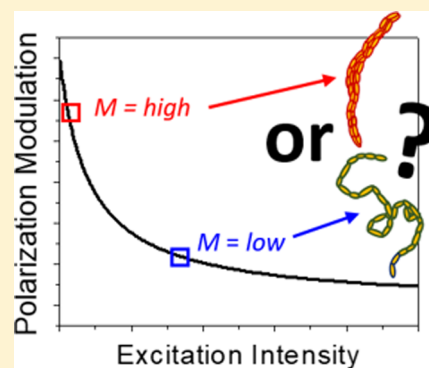


# Complex Photophysical Behaviors Affect Single Conjugated Molecule Optical Anisotropy Measurements

Heungman Park,<sup>†,‡,§</sup> Youngah Kwon,<sup>†,§</sup> and Laura J. Kaufman<sup>\*,†</sup><sup>†</sup>Department of Chemistry, Columbia University, New York, New York 10027, United States<sup>‡</sup>Department of Physics and Astronomy, Texas A&M University-Commerce, Commerce, Texas 75428, United States**S** Supporting Information

**ABSTRACT:** Polarization modulation depth ( $M$ ) measurements have been widely used as a technique to report on transition dipole alignment and thus molecular conformation of single conjugated polymers and aggregates. Such extrapolation of conformation from these measurements, however, is complicated by the fact that photophysical processes (which themselves are coupled to conformation) may influence  $M$  values. Here, we show that the presence of intensity-dependent partial photoluminescence quenching can suppress  $M$  values, with this suppression more prominent in molecules with highly aligned transition dipoles. We show that these findings on  $M$  values are a direct consequence of behaviors of fluorescence intensity maxima and minima as a function of excitation polarization in poly[2-methoxy-5-(2-ethylhexyloxy)-1,4-phenylenevinylene] single molecules, as supported by a simulation that reproduces the experimental results. Our findings show that interpreting  $M$  values of molecules with complex photophysics should be done with caution.

**■ INTRODUCTION**

Optical anisotropy measurements have been widely used to characterize a variety of single molecules.<sup>1–12</sup> Among these techniques, fluorescence polarization modulation depth ( $M$ ) measurements have been commonly applied to ascertain information on the conformation of single conjugated polymers and aggregates.<sup>13–28</sup> Although it is conceptually simple to understand why modulation depth measurements are closely connected to degree of alignment of transition dipoles and thus physical anisotropy of an interrogated molecule or aggregate, the interpretation of the value may be challenging, particularly in systems with complex photophysical behavior. Attempts to validate and strengthen information obtained from  $M$  measurements have come in the form of side-by-side experiment and modeling as well as experimental variations, in which both excitation and emission  $M$  values are measured.<sup>28–32</sup> Recently, we investigated how monitoring  $M$  values during photobleaching could reveal whether more compact or extended regions of the prototypical conjugated polymer poly[2-methoxy-5-(2-ethylhexyloxy)-1,4-phenylenevinylene] (MEH-PPV) were more photostable;<sup>26</sup> this work also clearly showed how partial photobleaching (and number of absorbing chromophores) itself affects measured  $M$  value for a molecule with static conformation. Here, we investigate a similar phenomenon, showing how  $M$  values may be suppressed in the presence of quenching processes, including those that have been suggested to be significant exciton quenching and de-excitation mechanisms in MEH-PPV.<sup>33–42</sup> This phenomenon is analogous to one observed and described previously in bulk fluorescence anisotropy measurements on J-aggregates.<sup>43,44</sup>

Modulation depth can be measured by monitoring intensity of photoluminescence (PL) as a function of excitation and/or emission light polarization angle. In this study, excitation light polarization is modulated.  $M$  is typically defined as the normalized difference between the maximum and minimum intensities ( $I_{\max}$  and  $I_{\min}$ , respectively) of the PL curve as a function of light polarization

$$M = \frac{I_{\max} - I_{\min}}{I_{\max} + I_{\min}} = \frac{A}{I_{\text{ave}}} \quad (1)$$

where  $A$  is the amplitude of a sinusoidal modulation and  $I_{\text{ave}}$  is the mean intensity of the modulated signals (Figure 1a). Typically, modulation depth is obtained by fitting the PL curve as a function of polarization angle to

$$I_{\text{PL}} = C[1 + M \cos\{2(\varphi - \varphi_0)\}] \quad (2)$$

with  $I_{\text{PL}}$  the intensity of photoluminescence,  $\varphi$  the polarization angle of the excitation light,  $\varphi_0$  a reference polarization angle corresponding to the maximum intensity angle of the excitation polarization, and  $C$  a proportionality constant.

In conjugated polymers, absorption of photons is followed by creation of excitons, tightly bound electron–hole pairs. Even in single conjugated polymers, multiple excitons may be generated, and these may migrate to local minimum energy sites at which emission may occur. Such emission sites may

Received: November 9, 2018

Revised: December 20, 2018

Published: January 2, 2019

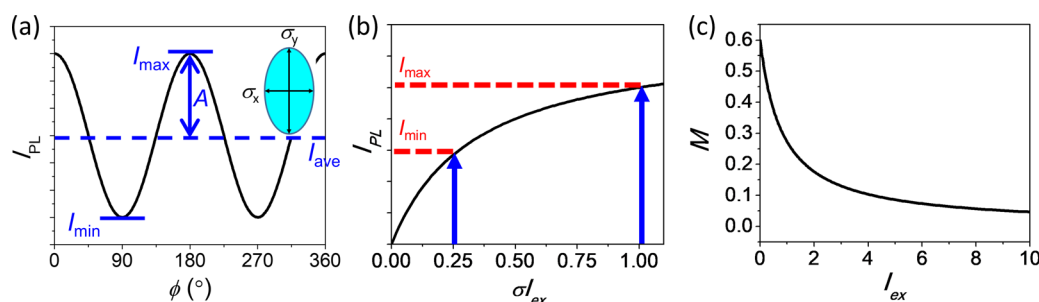


**Figure 1.** (a) Photoluminescence modulation curve used to calculate  $M$  for a simulated molecule with absorption cross-sections projected onto the sample plane of  $\sigma_x = 0.25$  and  $\sigma_y = 1.0$  (inset), with  $I_{\min}$ ,  $I_{\max}$ ,  $I_{\text{ave}}$ , and  $A$  as in eq 1. (b) PL intensity as a function of excitation intensity ( $I_{\text{ex}}$ ) for the example molecule described in (a) and with  $\alpha = 10$ ,  $\beta = 3$  according to eq 3. (c) Modulation depth ( $M$ ) vs excitation intensity for the example molecule as defined by eq 4.

become dark either permanently after chromophores are affected by photobleaching or temporarily, when an exciton occupies a long-lived state such as a triplet. Another mechanism by which temporary extinction of emission may occur is exciton–exciton annihilation. For multichromophoric conjugated polymers, exciton–exciton annihilation is expected to increase as a function of excitation intensity and polymer molecular weight.<sup>32,45</sup> Indeed, excitation intensity-dependent photoluminescence measurements showed that many conjugated polymer materials exhibit exciton–exciton annihilation and result in quenching at excitation power densities at and above  $\approx 0.1 \text{ W/cm}^2$  at  $\lambda = 458 \text{ nm}$ .<sup>39</sup> On the single-molecule level, this was shown for poly(3-hexylthiophene) (P3HT), where the PL increase deviates from a linear correlation with an excitation intensity  $\approx 50 \text{ W/cm}^2$  at  $\lambda = 485 \text{ nm}$ .<sup>45</sup>

Here, we consider how complex photophysical processes affect measured modulation depth using intensity-dependent exciton–exciton annihilation to illustrate the point. For both single and multichromophoric single polymers with exciton migration and intensity-dependent annihilation, PL intensity can be expressed by

$$I_{\text{PL}} = \frac{\alpha}{1 + \beta\sigma I_{\text{ex}}} \sigma I_{\text{ex}} \quad (3)$$

where  $\alpha$  is a proportionality factor related to internal quantum efficiency,  $\sigma$  is absorption cross-section, and  $\beta$  is a quenching factor.<sup>45</sup> In single P3HT molecules, it was shown that this form described observed PL intensity, consistent with singlet–triplet annihilation.<sup>45</sup> Although eq 3 was used to describe molecular weight- and excitation intensity-dependent saturation in single P3HT molecules presumed to funnel all excitons to a single emitting site, this model can also serve as an effective expression for photoluminescence in molecules with multiple exciton domains such as MEH-PPV. In this case, in the absence of exciton domain coupling, quenching would occur in accordance with eq 3 within each exciton domain, and the total photoluminescence intensity would be a sum of that from all domains, each described by eq 3. This model would then be appropriate both for MEH-PPV molecules in ordered, collapsed conformations (with high  $M$  and few exciton domains) and those in more extended conformations (with low  $M$  and a greater number of exciton domains). More generally, we note that eq 3 can describe quenching processes beyond singlet–triplet annihilation, and such quenching can emerge from a number of processes that involve exciton migration to long-lived quenching sites such as defects and charge traps.<sup>36</sup>

Within the model characterized by eq 3, in the absence of quenching ( $\beta = 0$ ), PL intensity is directly proportional to the absorption cross-section. For a molecule with  $\sigma_x = 0.25$  and  $\sigma_y = 1.0$ , following from eqs 1 and 3,  $M = (\sigma_y - \sigma_x)/(\sigma_y + \sigma_x) = 0.6$ , independent of excitation intensity. However, if  $\beta$  is nonzero and quenching occurs,  $M$  will be excitation intensity-dependent (except for molecules with  $M = 0$  and 1) and assuming  $\alpha$  and  $\beta$  are polarization independent, will vary as

$$M = \frac{\sigma_y - \sigma_x}{\sigma_x + \sigma_y + 2\beta\sigma_x\sigma_y I_{\text{ex}}} \quad (4)$$

For  $M'$  measured at an excitation intensity  $cI_{\text{ex}}$ , with  $c$  greater than 1,  $M' < M$  for the same molecule in the same conformation, and

$$M' = \frac{\sigma_x + \sigma_y + 2\beta\sigma_x\sigma_y I_{\text{ex}}}{\sigma_x + \sigma_y + 2c\beta\sigma_x\sigma_y I_{\text{ex}}} \times M \quad (5)$$

The value of  $M'$  can also be expressed through a generalized form of eq 1, via

$$M' = \frac{aI_{\text{max}} - bI_{\text{min}}}{aI_{\text{max}} + bI_{\text{min}}} \quad (6)$$

If there is no excitation intensity-dependent quenching, coefficients  $a$  and  $b$  will be identical and  $M' = M$ . However, if more quenching occurs at a higher excitation intensity,  $a < b$  and  $M' < M$ . Assuming that  $\alpha$  and  $\beta$  in eq 3 are equal along the orthogonal  $x$  and  $y$  orientations of the molecule,  $\alpha = 10$ , and  $\beta = 3$  in a molecule with  $\sigma_x = 0.25$  and  $\sigma_y = 1.0$ , the  $M$  value will decrease from 0.54 to 0.27 for a relative excitation intensity increase of a factor of 10 ( $I_{\text{ex}} = 0.1$ – $1.0$ ) (Figure 1b,c). At low excitation intensity, PL intensity increases nearly linearly with excitation intensity, quenching is negligible, and the  $M$  value is close to 0.6. As excitation intensity reaches the regime in which quenching is evident,  $M$  falls rather rapidly to values typically associated with molecules lacking significant optical anisotropy. Such an excitation intensity-dependent  $M$  value change will be observed if emission intensity saturates with respect to increasing excitation intensity, regardless of particular source of quenching.

In this paper, we confirm the effect of excitation intensity-dependent quenching on modulation depth measurements of single conjugated molecules with multiple exciton domains. The model system used is MEH-PPV single molecules dissolved in chloroform and confined in polystyrene since such molecules typically show broad  $M$  distributions,<sup>26</sup> which

allows us to understand the effect as a function of initially measured modulation depth.

## EXPERIMENT

MEH-PPV of  $M_n = 140$  kDa and polydispersity index (PDI) = 1.8 was purchased from Polymer Source and was used without further purification. The MEH-PPV was diluted in  $\approx 4$  wt % polystyrene ( $M_w = 6.4$  kDa, PDI = 1.05) with chloroform as the solvent. The solution was spin-cast onto native oxide-covered silicon wafers to prepare films of  $\approx 200$  nm thickness. The concentration of MEH-PPV in the solution was  $\approx 10^{-11}$  M, and the average separation between molecules in the films was greater than  $1 \mu\text{m}$  when imaged with wide-field microscopy. A home-built wide-field epi-fluorescence microscope system was used to perform the experiments. Samples were placed in a vacuum cryostat held at  $\approx 1$  mTorr. A continuous wave laser at 532 nm (Spectra Physics; Millennia V, Nd:vanadate 532 nm diode laser) was the excitation source. Circularly polarized light was used for the excitation intensity-dependent PL measurement. Excitation intensity was increased from  $20 \text{ W/cm}^2$  in increments of  $20 \text{ W/cm}^2$  until excitation intensity reached  $200 \text{ W/cm}^2$ . Excitation intensity was then decreased in increments of  $20 \text{ W/cm}^2$  until it reached the starting point of  $20 \text{ W/cm}^2$ . Ten frames were collected for each measurement at a frame rate of 5 Hz. The 10 frame average PL intensity was used for further data analysis. For  $M$  measurements, a rotating linear polarizer was placed before the objective lens (Zeiss, LD Plan-Neofluar, air 63 $\times$ , NA = 0.75, WD = 1.5 mm) and was rotated at a rate of  $10^\circ/\text{s}$ . Each  $M$  measurement took 36 s. Excitation modulation depth values of MEH-PPV molecules were obtained with a home-written Python program that fit the modulation depth data to eq 2. More detailed data analysis procedures are outlined in ref 26 as well as in the Supporting Information.

## RESULTS AND DISCUSSION

First, circularly polarized excitation light was used to measure PL intensity of a set of single MEH-PPV molecules as a function of excitation intensity from 20 to  $200 \text{ W/cm}^2$ , which is within the range of typical single-molecule experiments (Figure 2a). The results indicate that significant PL quenching occurs at high excitation intensities, consistent with previous work.<sup>39</sup> However, we also note that there is significant

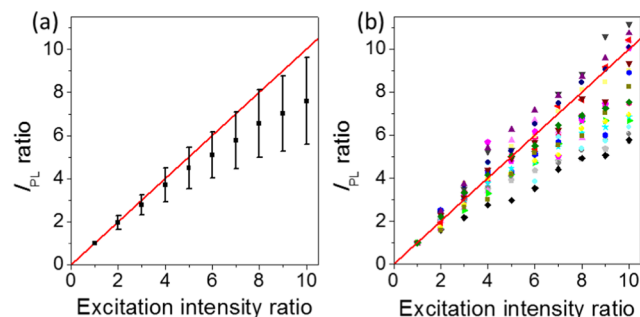


**Figure 2.** (a) Photoluminescence intensity ratio as a function of excitation intensity ratio for MEH-PPV molecules dissolved in chloroform and immobilized in PS ( $n = 193$ ). The reference excitation intensity is  $20 \text{ W/cm}^2$ . Error bars indicate the standard deviations of the PL intensities. (b) Data from 20 single molecules selected at random from the results shown in (a). Red line ( $y = x$ ) is a guide to the eye.

molecule-to-molecule variation in the quenching curves, which is evident in the error bars that represent standard deviation of the PL intensities, with particular molecules showing consistent behavior as a function of increasing excitation intensity (Figure 2b). The molecule-to-molecule variations may emerge from differences in quenching as a function of molecular conformation. There may also be (potentially conformation-dependent) photoactivation processes that compete with the quenching processes, as is evident from particular molecules whose PL intensity increases superlinearly with excitation intensity (Figure 2b). Partial photobleaching, which has also been shown to affect measured polarization modulation values,<sup>26</sup> is not at play, as only molecules with the same PL intensity as excitation power was ramped up and then down were analyzed, thus excluding those molecules exhibiting photobleaching during the experiment.

The intensity-dependent quenching shown in Figure 2 suggests that the quenching effects on  $M$  values described in the Introduction may occur in these molecules. This is supported by polarization modulation measurements at different excitation intensities performed on these same molecules (Figure 3). Some molecules represented in the

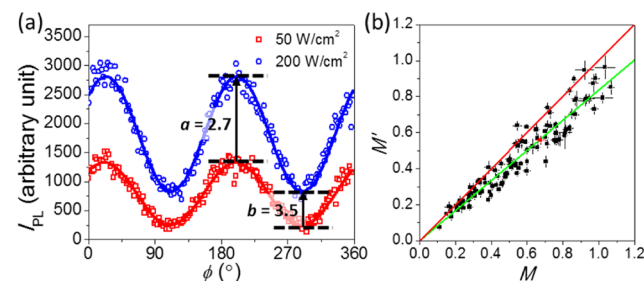


**Figure 3.** (a) PL intensity as a function of polarization angle of excitation intensity for a single MEH-PPV molecule at  $50 \text{ W/cm}^2$  (red) and  $200 \text{ W/cm}^2$  (blue). Relative  $I_{\text{max}}$  (co-efficient  $a$  in eq 6) (2.7) and  $I_{\text{min}}$  (co-efficient  $b$  in eq 6) (3.5) values are shown. Lines are fits to the raw data (symbols) that are used to obtain the values of  $M = 0.68$  ( $I_{\text{ex}} = 50 \text{ W/cm}^2$ ) and  $M = 0.54$  ( $I_{\text{ex}} = 200 \text{ W/cm}^2$ ) via eq 2. (b) A scatter plot of  $M$  values (measured at  $I_{\text{ex}} = 50 \text{ W/cm}^2$ ) and  $M'$  values (measured at  $I_{\text{ex}} = 200 \text{ W/cm}^2$ ) for  $n = 111$  molecules. The red point is the molecule shown in (a). Error bars represent fit uncertainty. The red line is a guide to the eye with  $y = x$ . The green line is a linear fit to the data with slope = 0.84.

intensity-dependent measurements (Figure 2a) were excluded from the analysis represented by Figure 3: these molecules exhibited photoblinking and/or complete photobleaching during the polarization modulation measurements. A representative dataset is shown in Figure 3a: for two excitation powers that vary by a factor of 4.0, the increase in the ratio of  $I_{\text{max}}$  ( $=2.7$ ) is less than that in  $I_{\text{min}}$  ( $=3.5$ ). As a result, the measured  $M$  value decreases from 0.68 to 0.54. A scatter plot of  $M$  and  $M'$  values for each MEH-PPV molecule measured at  $I_{\text{ex}} = 50 \text{ W/cm}^2$  ( $M$ ) and  $200 \text{ W/cm}^2$  ( $M'$ ) is shown in Figure 3b. Nearly, all  $M'$  values are lower than the  $M$  value for the same molecule, with the data well fit by a line with slope of 0.84.

To confirm that photobleaching is not at play and that measurement to measurement variation is not responsible for the observed decrease of  $M$  with increasing excitation intensity,  $M$  values were measured a second time at  $50 \text{ W/cm}^2$  after the high intensity  $M'$  measurements were performed. In this case, the best-fit line has a slope of 1.01 (Figure S1), confirming that

the tendency toward lower  $M$  values at high excitation intensity is not related to photobleaching or noise. To further analyze individual molecules' response, co-efficients  $a$  and  $b$  as defined in eq 6 and the ratio  $a/b$  are plotted with respect to  $M$  values in Figure 4. The data show that higher  $M$  molecules have lower

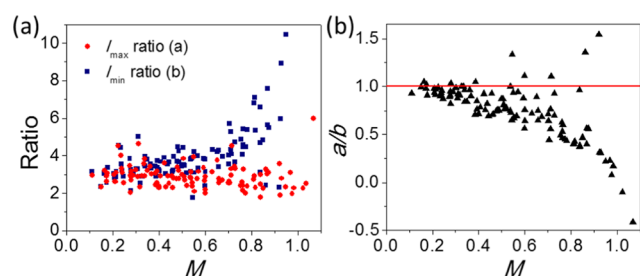


**Figure 4.** (a) Scatter plots of  $I_{\max}$  ratio (co-efficient  $a$  in eq 6) and  $I_{\min}$  ratio (co-efficient  $b$  in eq 6) vs  $M$  for the set of molecules also shown in Figure 3. (b) Scatter plot of  $a/b$  vs  $M$ . Several data points are outside the range shown for  $a/b$ .

$a/b$  ratios, consistent with the greater decrease in polarization modulation as a function of excitation intensity compared to molecules with low  $M$  values (Figure 3). Closer inspection of the data shows that  $a/b < 1$  for most molecules, as expected. However, the change in the  $a/b$  ratio is driven not only by a decrease in  $a$  that increases as  $M$  increases but also by an increase in  $b$ , with many molecules with high  $M$  showing  $b$  ratios greater than 4, the expected ratio if no quenching was present. Molecules with high  $M$  values necessarily have a small value of  $I_{\min}$ , thus increasing the chance that noise plays a role in changes of this value as a function of conditions.

To characterize how noise may manifest in these measurements, we performed simulations as detailed in the Supporting Information. Briefly, 1000 molecules were simulated to generate an  $M$  distribution consistent with the experimental distribution. Following that, both noise and quenching were considered independently for their influence on measured  $M$  values as a function of excitation intensity. Figure S2 shows that, as expected, in the absence of noise and any photophysical processes such as exciton–exciton annihilation, measurements of  $M$  at two different excitation intensities are identical (Figure S2a,b). The addition of noise affects the results, with the  $I_{\max}$  ratio (co-efficient  $a$ ) and  $I_{\min}$  ratio (co-efficient  $b$ ) both broadening (Figure S2c). This is more apparent and  $M$  dependent for  $I_{\min}$ , as expected due to the sensitivity of low  $I_{\min}$  values to noise, which leads to unphysical  $I_{\min}$  ratios, including negative values and very high positive values of this quantity compared to the expected value of 4. However, in contrast to the experimental data, the spread in  $I_{\max}$  and  $I_{\min}$  ratios is rather symmetric, such that the best-fit line for the simulated  $M'$  vs  $M$  scatter plot retains a best-fit slope of near 1 (slope = 0.99) (Figure S2d).

When exciton quenching is included in the (noise-free) simulation, sublinear changes of  $I_{\min}$  and  $I_{\max}$  with excitation intensity are evident (Figure S2e). Beyond that,  $I_{\min}$  values increase with increasing  $M$ , consistent with the experimental data. Incorporating photoinduced quenching according to eq 3 with  $\beta = 2$  best captures the  $I_{\max}$  suppression seen experimentally. Although this inclusion of quenching also reproduces some aspects of the experimental  $M'$  vs  $M$  measurements shown in Figure 3, as discussed in the Introduction, intensity-independent  $M$  values will be present

at 0 and 1 even in the presence of quenching (Figure S2f). Due to the tendency for molecules with high  $M$  values to be more strongly affected by noise, adding noise to these simulations including photoquenching recovers the observed behaviors of  $I_{\min}$ ,  $I_{\max}$ , and  $M'$  vs  $M$ , with the simulated results showing a slope of 0.84 (Figure 5).

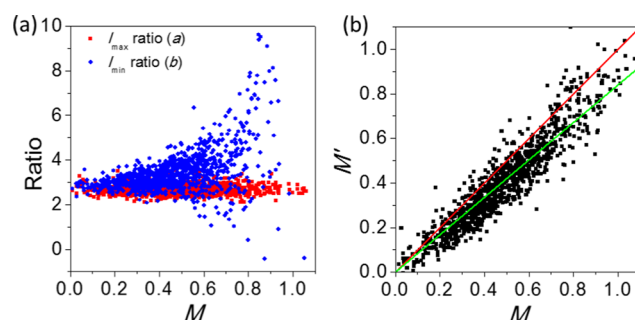


**Figure 5.** (a) Scatter plots of  $I_{\max}$  ratio and  $I_{\min}$  ratio as defined in eq 6 vs  $M$  for a simulation of 1000 molecules with noise and quenching as described in the Supporting Information and an excitation intensity ratio of 4, as in the experiment. (b)  $M'$  vs  $M$  for the simulation also depicted in (a). The red line is a guide to the eye, showing  $y = x$ . The green line is a linear fit to the data with slope = 0.84.

Although the measured  $M$  suppression at high excitation intensity is consistent with the simulated results, additional photophysics beyond that captured with the quenching described by eq 3 could also be at play. For example, photoactivation processes are sometimes evident in single-molecule data, with a given molecule becoming brighter over time at a given illumination intensity. Although molecules with strong evidence of such behavior were not present in this dataset (see Figure S1), some do display photoactivation with increasing intensity (Figure 2b). Beyond photoactivation, MEH-PPV displays a broad range of photophysics that may not be captured by eq 3 and may further be conformation dependent.<sup>34,36,39</sup> Indeed, one may expect the assumption of independent exciton domains to preferentially fail in MEH-PPV molecules with more compact conformation, where efficient exciton funneling exists. Further experimental measurements and theoretical treatment would be needed to clarify these issues; however, our experimental data suggest that MEH-PPV molecules with a range of conformations display photoquenching behavior and subsequent intensity-dependent  $M$  values captured by the relatively simple model originally used to characterize intensity-dependent quenching through singlet–triplet annihilation.

## CONCLUSIONS

Modulation depth measurements are widely used to determine the degree of anisotropy and conformation of emitting conjugated polymers at the single-molecule and aggregate levels. However, many such materials exhibit complex photophysics, including strong evidence of excitation intensity-dependent photoquenching. We show here that intensity-dependent quenching that manifests in sublinear photoluminescence intensity growth with increasing excitation intensity results in decreasing  $M$  values as a function of increasing excitation intensity, demonstrating that interpretation of  $M$  values and changes thereof must be done with caution and should not immediately be attributed to differences in molecular conformation. Beyond the intensity-

dependent singlet–triplet annihilation modeled here, other intensity-dependent photophysics may affect measured  $M$  values, and additional experimental and theoretical work are required to fully clarify origins of intensity-dependent polarization modulation in multichromophoric molecules with complex photophysics such as MEH-PPV.

## ■ ASSOCIATED CONTENT

### ■ Supporting Information

The Supporting Information is available free of charge on the ACS Publications website at DOI: 10.1021/acs.jpcc.8b10916.

Data analysis and simulations;  $M$  measurements at low intensity before and after high intensity measurements;  $I_{\min}$ ,  $I_{\max}$ , and  $M'$  vs  $M$  for simulations with neither noise nor photoquenching, only noise, and only photoquenching (PDF)

## ■ AUTHOR INFORMATION

### Corresponding Author

\*E-mail: kaufman@chem.columbia.edu.

### ORCID

Laura J. Kaufman: 0000-0002-3754-0831

### Author Contributions

<sup>§</sup>H.P. and Y.K.K. contributed equally to this work.

### Notes

The authors declare no competing financial interest.

## ■ ACKNOWLEDGMENTS

The authors acknowledge support from National Science Foundation grants CHE 1660392 and CHE 1807931. We thank Jaesung Yang for helpful discussions.

## ■ REFERENCES

- (1) Ha, T.; Enderle, T.; Chemla, D. S.; Selvin, P. R.; Weiss, S. Single Molecule Dynamics Studied by Polarization Modulation. *Phys. Rev. Lett.* **1996**, *77*, 3979–3982.
- (2) Ha, T.; Laurence, T. A.; Chemla, D. S.; Weiss, S. Polarization Spectroscopy of Single Fluorescent Molecules. *J. Phys. Chem. B* **1999**, *103*, 6839–6850.
- (3) Harms, G. S.; Sonnleitner, M.; Schütz, G. J.; Gruber, H. J.; Schmidt, T. Single-Molecule Anisotropy Imaging. *Biophys. J.* **1999**, *77*, 2864–2870.
- (4) Gradinaru, C. C.; Marushchak, D. O.; Samim, M.; Krull, U. J. Fluorescence Anisotropy: From Single Molecules to Live Cells. *Analyst* **2010**, *135*, 452–459.
- (5) Ebihara, Y.; Vacha, M. Relating Conformation and Photophysics in Single MEH-PPV Chains. *J. Phys. Chem. B* **2008**, *112*, 12575–12578.
- (6) Furumaki, S.; Habuchi, S.; Vacha, M. Fluorescence-Detected Three-Dimensional Linear Dichroism: A Method to Determine Absorption Anisotropy in Single Sub-Wavelength Size Nanoparticles. *Chem. Phys. Lett.* **2010**, *487*, 312–314.
- (7) Vacha, M.; Habuchi, S. Conformation and Physics of Polymer Chains: A Single-Molecule Perspective. *NPG Asia Mater.* **2010**, *2*, 134–142.
- (8) Furumaki, S.; Vacha, F.; Habuchi, S.; Tsukatani, Y.; Bryant, D. A.; Vacha, M. Absorption Linear Dichroism Measured Directly on a Single Light-Harvesting System: The Role of Disorder in Chlorosomes of Green Photosynthetic Bacteria. *J. Am. Chem. Soc.* **2011**, *133*, 6703–6710.
- (9) Kobayashi, H.; Onda, S.; Furumaki, S.; Habuchi, S.; Vacha, M. A Single-Molecule Approach to Conformation and Photophysics of Conjugated Polymers. *Chem. Phys. Lett.* **2012**, *528*, 1–6.
- (10) Huser, T.; Yan, M.; Rothberg, L. J. Single Chain Spectroscopy of Conformational Dependence of Conjugated Polymer Photophysics. *Proc. Natl. Acad. Sci. U.S.A.* **2000**, *97*, 11187–11191.
- (11) Warshaw, D. M.; Hayes, E.; Gaffney, D.; Lauzon, A.-M.; Wu, J.; Kennedy, G.; Trybus, K.; Lowey, S.; Berger, C. Myosin Conformational States Determined by Single Fluorophore Polarization. *Proc. Natl. Acad. Sci. U.S.A.* **1998**, *95*, 8034–8039.
- (12) Ying, L.; Xie, X. S. Fluorescence Spectroscopy, Exciton Dynamics, and Photochemistry of Single Allophycocyanin Trimers. *J. Phys. Chem. B* **1998**, *102*, 10399–10409.
- (13) Hu, D.; Yu, J.; Wong, K.; Bagchi, B.; Barbara, P. F.; Rossky, P. J. Collapse of Stiff Conjugated Polymers with Chemical Defects into Ordered, Cylindrical Conformations. *Nature* **2000**, *405*, 1030–1033.
- (14) Vogelsang, J.; Adachi, T.; Brazard, J.; Vanden Bout, D. A.; Barbara, P. F. Self-Assembly of Highly Ordered Conjugated Polymer Aggregates with Long-Range Energy Transfer. *Nat. Mater.* **2011**, *10*, 942–946.
- (15) Adachi, T.; Brazard, J.; Ono, R. J.; Hanson, B.; Traub, M. C.; Wu, Z. Q.; Li, Z.; Bolinger, J. C.; Ganesan, V.; Bielawski, C. W.; et al. Regioregularity and Single Polythiophene Chain Conformation. *J. Phys. Chem. Lett.* **2011**, *2*, 1400–1404.
- (16) Thiessen, A.; Vogelsang, J.; Adachi, T.; Steiner, F.; Vanden Bout, D. A.; Lupton, J. M. Unraveling the Chromophoric Disorder of Poly(3-Hexylthiophene). *Proc. Natl. Acad. Sci. U.S.A.* **2013**, *110*, E3550–E3556.
- (17) Vogelsang, J.; Lupton, J. M. Solvent Vapor Annealing of Single Conjugated Polymer Chains: Building Organic Optoelectronic Materials from the Bottom Up. *J. Phys. Chem. Lett.* **2012**, *3*, 1503–1513.
- (18) Chen, P. Y.; Rassamesard, A.; Chen, H. L.; Chen, S.-A. Conformation and Fluorescence Property of Poly(3-Hexylthiophene) Isolated Chains Studied by Single Molecule Spectroscopy: Effects of Solvent Quality and Regioregularity. *Macromolecules* **2013**, *46*, 5657–5663.
- (19) Hu, Z.; Adachi, T.; Haws, R. T.; Shuang, B.; Ono, R. J.; Bielawski, C. W.; Landes, C. F.; Rossky, P. J.; Vanden Bout, D. A. Excitonic Energy Migration in Conjugated Polymers: The Critical Role of Interchain Morphology. *J. Am. Chem. Soc.* **2014**, *136*, 16023–16031.
- (20) Traub, M. C.; Dubay, K. H.; Ingle, S. E.; Zhu, X.; Plunkett, K. N.; Reichman, D. R.; Vanden Bout, D. A. Chromophore-Controlled Self-Assembly of Highly Ordered Polymer Nanostructures. *J. Phys. Chem. Lett.* **2013**, *4*, 2520–2524.
- (21) Traub, M. C.; Vogelsang, J.; Plunkett, K. N.; Nuckolls, C.; Barbara, P. F.; Vanden Bout, D. A. Unmasking Bulk Exciton Traps and Interchain Electronic Interactions with Single Conjugated Polymer Aggregates. *ACS Nano* **2012**, *6*, 523–529.
- (22) Stangl, T.; Wilhelm, P.; Remmersen, K.; Höger, S.; Vogelsang, J.; Lupton, J. M. Mesoscopic Quantum Emitters from Deterministic Aggregates of Conjugated Polymers. *Proc. Natl. Acad. Sci. U.S.A.* **2015**, *112*, E5560–E5566.
- (23) Yang, J.; Park, H.; Kaufman, L. J. Highly Anisotropic Conjugated Polymer Aggregates: Preparation and Quantification of Physical and Optical Anisotropy. *J. Phys. Chem. C* **2017**, *121*, 13854–13862.
- (24) Hu, Z.; Haws, R. T.; Fei, Z.; Boufflet, P.; Heeney, M.; Rossky, P. J.; Vanden Bout, D. A. Impact of Backbone Fluorination on Nanoscale Morphology and Excitonic Coupling in Polythiophenes. *Proc. Natl. Acad. Sci. U.S.A.* **2017**, *114*, 5113–5118.
- (25) Yang, J.; Park, H.; Kaufman, L. J. In Situ Optical Imaging of the Growth of Conjugated Polymer Aggregates. *Angew. Chem., Int. Ed.* **2018**, *57*, 1826–1830.
- (26) Park, H.; Hoang, D. T.; Paeng, K.; Yang, J.; Kaufman, L. J. Conformation-Dependent Photostability among and within Single Conjugated Polymers. *Nano Lett.* **2015**, *15*, 7604–7609.
- (27) Thomsson, D.; Lin, H.; Scheblykin, I. G. Correlation Analysis of Fluorescence Intensity and Fluorescence Anisotropy Fluctuations in Single-Molecule Spectroscopy of Conjugated Polymers. *ChemPhysChem* **2010**, *11*, 897–904.

(28) Mirzov, O.; Bloem, R.; Hania, P. R.; Thomsson, D.; Lin, H.; Scheblykin, I. G. Polarization Portraits of Single Multichromophoric Systems: Visualizing Conformation and Energy Transfer. *Small* **2009**, *5*, 1877–1888.

(29) Hu, D.; Yu, J.; Wong, K.; Bagchi, B.; Barbara, P. F.; Rossky, P. J. Collapse of Stiff Conjugated Polymers with Chemical Defects into Ordered, Cylindrical Conformations. *Nature* **2000**, *405*, 1030–1033.

(30) Traub, M. C.; Lakhwani, G.; Bolinger, J. C.; Vanden Bout, D. A.; Barbara, P. F. Electronic Energy Transfer in Highly Aligned MEH-PPV Single Chains. *J. Phys. Chem. B* **2011**, *115*, 9941–9947.

(31) Adachi, T.; Lakhwani, G.; Traub, M. C.; Ono, R. J.; Bielawski, C. W.; Barbara, P. F.; Vanden Bout, D. A. Conformational Effect on Energy Transfer in Single Polythiophene Chains. *J. Phys. Chem. B* **2012**, *116*, 9866–9872.

(32) Camacho, R.; Thomsson, D.; Sforazzini, G.; Anderson, H. L.; Scheblykin, I. G. Inhomogeneous Quenching as a Limit of the Correlation between Fluorescence Polarization and Conformation of Single Molecules. *J. Phys. Chem. Lett.* **2013**, *4*, 1053–1058.

(33) Hale, G. D.; Oldenburg, S. J.; Halas, N. J. Observation of Triplet Exciton Dynamics in Conjugated Polymer Films Using Two-Photon Photoelectron Spectroscopy. *Phys. Rev. B* **1997**, *55*, R16069–R16071.

(34) Yu, J.; Lammi, R.; Gesquiere, A. J.; Barbara, P. F. Singlet–Triplet and Triplet–Triplet Interactions in Conjugated Polymer Single Molecules. *J. Phys. Chem. B* **2005**, *109*, 10025–10034.

(35) Barbara, P. F.; Gesquiere, A. J.; Park, S.-J.; Lee, Y. J. Single-Molecule Spectroscopy of Conjugated Polymers. *Acc. Chem. Res.* **2005**, *38*, 602–610.

(36) Scheblykin, I. G.; Yartsev, A.; Pullerits, T.; Gulbinas, V.; Sundström, V. Excited State and Charge Photogeneration Dynamics in Conjugated Polymers. *J. Phys. Chem. B* **2007**, *111*, 6303–6321.

(37) Hou, L.; Adhikari, S.; Tian, Y.; Scheblykin, I. G.; Orrit, M. Absorption and Quantum Yield of Single Conjugated Polymer Poly[2-Methoxy-5-(2-Ethylhexyloxy)-1,4-Phenylenevinylene] (MEH-PPV) Molecules. *Nano Lett.* **2017**, *17*, 1575–1581.

(38) Hader, K.; Consani, C.; Brixner, T.; Engel, V. Mapping of Exciton–exciton Annihilation in MEH-PPV by Time-Resolved Spectroscopy: Experiment and Microscopic Theory. *Phys. Chem. Chem. Phys.* **2017**, *19*, 31989–31996.

(39) Sahoo, D.; Tian, Y.; Sforazzini, G.; Anderson, H. L.; Scheblykin, I. G. Photo-Induced Fluorescence Quenching in Conjugated Polymers Dispersed in Solid Matrices at Low Concentration. *J. Mater. Chem. C* **2014**, *2*, 6601–6608.

(40) Hooley, E. N.; Tilley, A. J.; White, J. M.; Ghiggino, K. P.; Bell, T. D. M. Energy Transfer in PPV-Based Conjugated Polymers: A Defocused Widefield Fluorescence Microscopy Study. *Phys. Chem. Chem. Phys.* **2014**, *16*, 7108–7114.

(41) Martini, I. B.; Smith, A. D.; Schwartz, B. J. Exciton-Exciton Annihilation and the Production of Interchain Species in Conjugated Polymer Films: Comparing the Ultrafast Stimulated Emission and Photoluminescence Dynamics of MEH-PPV. *Phys. Rev. B* **2004**, *69*, No. 035204.

(42) Barzykin, A. V.; Tachiya, M. Stochastic Model of Photo-dynamics in Multichromophoric Conjugated Polymers. *J. Phys. Chem. B* **2006**, *110*, 7068–7072.

(43) Juzeliūnas, G. Time-Dependent Fluorescence Depolarization Arising from Exciton Annihilation in Confined Molecular Domains. *Chem. Phys.* **1991**, *151*, 169–178.

(44) Scheblykin, I. G.; Varnavsky, O. P.; Bataiev, M. M.; Sliusarenko, O.; Van Der Auweraer, M.; Vitukhnovsky, A. G. Non-Coherent Exciton Migration in J-Aggregates of the Dye THIATS: Exciton-Exciton Annihilation and Fluorescence Depolarization. *Chem. Phys. Lett.* **1998**, *298*, 341–350.

(45) Steiner, F.; Vogelsang, J.; Lupton, J. M. Singlet-Triplet Annihilation Limits Exciton Yield in Poly(3-Hexylthiophene). *Phys. Rev. Lett.* **2014**, *112*, 1–5.